Porosity Effects of AlSi10mg Parts Produced by Selective Laser Melting

Noreriyanti Hasmuni, Mustaffa Ibrahim,*
Azli Amin Raus, Md Saidin Wahab, Khairu Kamarudin

Faculty of Mechanical and Manufacturing Engineering,
Universiti Tun Hussein Onn Malaysia, Parit Raja,
Batu Pahat, Johor, Malaysia

**yanti.hasmuni93@gmail.com*

ABSTRACT

Selective Laser Melting (SLM) is one of the powder-based manufacturing processes that has a wider established uses in the production of metallic alloy parts. It is capable of producing a high-density part through the melting of powder to form the desired shape. Fabrication of the AlSI10Mg part relies on several process parameters such as the laser power, laser scan speed, hatch distance, layer thickness and scanning strategy. They are specially designed and monitored to achieve optimum level. In this paper, porosity percentage were obtained from manipulating the hatch distance of fabricated SLM parts. The results appeared that smallest percentage obtained when the hatch distance was 0.13mm which is 0.46%. However, the highest porosity obtained when the lower hatch distance applied.

Keywords: *Additive manufacturing, Alsi10Mg, Selective Laser Melting, Porosity*

1. Introduction

SLM is one such process that is proficient in the field of AM since 2003. In SLM, a layer of powder material is first deposited onto a substrate of similar material composition as the powder material to ensure good bonding to the substrate surface. The laser then selectively scans across section predefined by the CAD file. The powder particles undergo melting and fuse together to form a solid thin layer of material forming the desired cross section. After

ISSN 1823- 5514, eISSN 2550-164X
Received for review: 2017-04-30
Accepted for publication: 2017-09-26
Published: 2018-03-15

this, a second layer of powder is deposited and the next cross section is scanned, joining it to the previous layer. This process repeats itself until the entire part is completed therefore obtaining a 3D physical part [1].

Because of the high degree of freedom offered by the additive manufacturing, parts having any possible geometry can theoretically be produced by SLM. More specifically, with this process it is possible to build parts with extremely complex shapes and geometries that would otherwise be difficult or impossible to produce using conventional manufacturing processes. The latest advances in the laser technology makes SLM devices are capable of melting and combining any type of material, including plastics, metals and ceramics. Recently, significant research activity has been focused on SLM processing of metallic materials. The materials studied include stainless and tool steels, with focus on the effect of the laser parameters on density, surface morphology and mechanical properties. [2].

The SLM process is controlled by the set of parameters illustrated in Figure 1 and Figure 2. The major build parameters involved in the process of selective laser melting are scanning speed, hatch distance, laser power and layer thickness. There are numerous investigations considering these parameters to enhance part density [3].

AlSi10Mg is a widely used casting alloy and is known for its good weldability and hardenability while maintaining a high thermal conductivity of 113 Wm^{-1} K^{-1} [4] Al alloys are of major interest for lightweight applications in aerospace and automotive sector. AlSi10Mg is an age-hardenable cast alloy with good mechanical properties. Castability and weldability is good due to the composition being close to eutectic Al-Si. Age hardening is enabled by Mg, which raises strength by Mg2Si precipitation sequence. Due to these reasons, AlSi10Mg is a good candidate for SLM. Process parameters resulting microstructure and mechanical properties have already been under thorough research for this alloy.[5]

Weingarten et al. studied the physical mechanism of the hydrogen pores in AlSi10Mg parts built by SLM, and the hydrogen porosity could be lowered by the efficient drying of the powder as well as modification of the SLM process parameters. Alloying magnesium to the Al-Si alloy enables the precipitation of Mg2Si phase, which significantly improves ductility and strengthens the matrix without compromising other mechanical properties. AlSi10Mg can be hardened through the precipitation of Mg2Si phase by a specified T6 heat treatment (solution with complete artificial aging) [6].

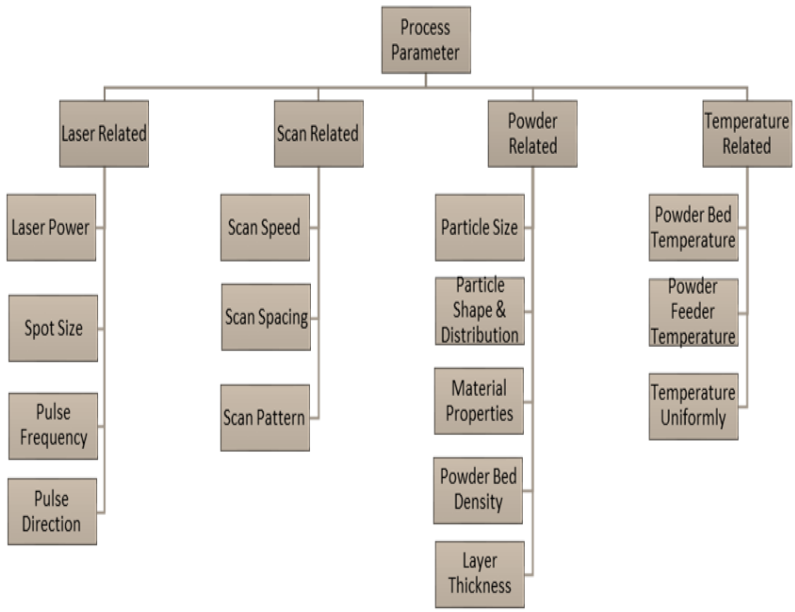

FIGURE 1: Process Parameter of SLM

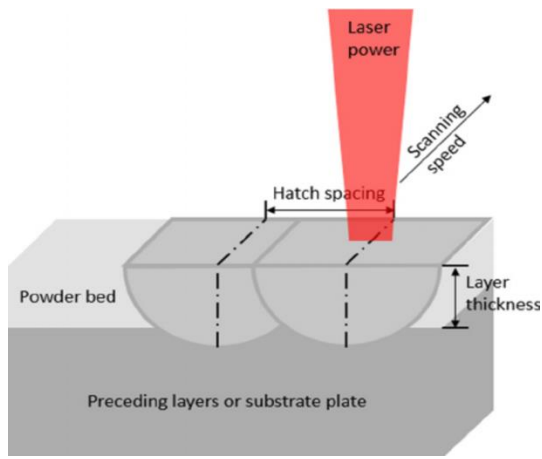

FIGURE 2 schematic diagrams of SLM process

2. Material and Experimental Work

a. Material

Besides the effect of processing parameters, the size, shape, particles distribution and chemical composition of the powder have a significant influence in the melting and fusing activity. The chemical composition of the AlSi10Mg powder which was supplied by LPW Technology Ltd is shown in Table I. In this research work, the powder was sowed on a double-sided carbon tape and softly shaken to assure a thin layer of powder being left on the sample block. The morphology and the size of the powder were examined using Field Emission Scanning Electron Microscope (FESEM, JSM-7600F) micrograph.

TABLE 1
Chemical composition of the investigated AlSi10Mg alloy (Wt. %)

Cu	Fe	Mg	N	Ni	Pb	O	Si	Ti	Zn	Al
0.05	0.10	0.39	0.20	0.01	0.01	0.11	10.00	0.15	0.10	bal

b. Experimental work

The SLM system SLM 125 HL (SLM Solutions), was used to manufacture all samples in this study. The machine system is equipped with a 400 W fibre laser with 80 µm laser beam spot and has a build chamber of 125 × 125 × 125 mm as shown in Figure 3. Argon is used as inert gas in the build chamber. The stripe scanning strategy with 45° orientation and 90° rotated incrementally no the next layer was used. The platform building was maintain at 150°c to avoid the build samples from warping due to non-uniform thermal expansion at elevated temperature. The thickness layer of the powder was constant at $30\mu m$ by lowering the build platform. An aluminium platform is placed on the building platform (XY table) and levelled [7].

FIGURE 3: Build chamber SLM system SLM125HL

This experiment was conducted by using the best setting parameters from previous study which is its laser power of 350 W and scan speed of 1650mm/s. Three sets of samples with dimensions of 10mm × 10mm × 10mm have been built to examine the microstructure of the top and side surface using optical microscope. Each sets comprising two surface which is top and side surface were manufacture by using three different hatch distance values 0.10mm, 0.13mm and 0.15mm. All samples were mounted, polished to 0.02 µm finish and electro-etched by tetrafluoroboric acid 48% in H2O.

2. Results and Discussions

Samples were analysed using an optical microscope with solutionDT software.

For each sample, 6 images were collected from the centre. Effect of changing the hatch spacing on the porosity content (porosity %) represented by the pore area fraction on micrographs determined using ImageJ Software.

E. Olankami [8] has reviewed that the density of the specimen mainly depends upon the hatch distance, composition and layer thickness whereas; hatch distance, layer thickness and laser power are the significant parameters which influence the porosity. However, G. Kasperovich [9] differ the statement with the hatch distance were the least influence the porosity of parts produced by SLM, compared to another parameter such as scanning speed and laser power. There were bunch of research about the scanning speed and laser power affects on the porosity of the parts produced by SLM, hence this study focusing only on hatching distance parameter [10][11].

The selection of the hatch distance is dictated by the width and depth shape of the scan track and the laser beam spot size, to ensure sufficient overlap so as to yield a consolidated part. Small hatch distances mean a

slower rate of production by increasing the primary time but allows more freedom in selecting the scan speed used. Large hatch distance will impose a limitation on the maximum layer thickness in which the part can be sliced thus increasing the auxiliary time.

The values of relative density data with hatching distance ranging from 0.1 mm to of 0.15 mm with intervals of 0.05 mm with laser power and scanning speed at 350 watt and 1650 mm /s constant respectively are shown in Figure 4, the preeminent result for the relative density was 99.34 % at hatching distance of 0.13 mm. After hatch distance of 0.13mm, the results showed inverse trends and it is because by increasing further it cause the reductions in the density of the material. [12]

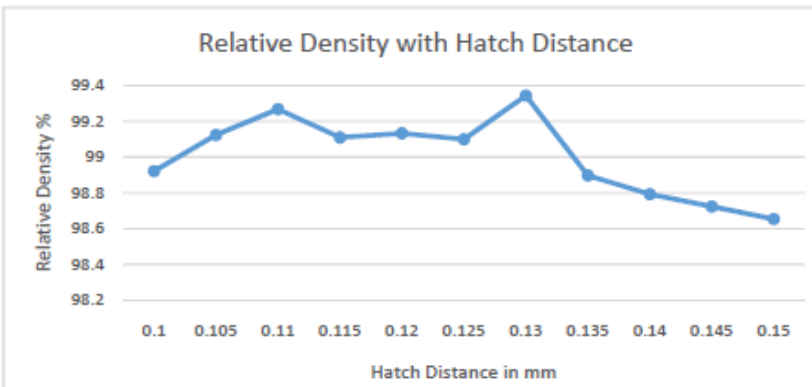

FIGURE 4: Relative Density with hatch distance [12].

The results obtained from ImageJ analysis software shows the hatch distance influence towards porosity of the parts produced. It is shown that only small percentage of porosity obtained. Table 2 belows shows the summary of the porosity % results deduced from ImageJ Software.

Table 2: Porosity % and average pores size deduced from ImageJ analysis software.

SET	SURFACE	LASER POWER (W)	SCANNING SPEED (mm/s)	HATCH DISTANCE (mm)	POROSITY %
1	TOP	350	1650	0.10	1.263
	SIDE	350	1650	0.10	1.475
2	TOP	350	1650	0.13	0.53
	SIDE	350	1650	0.13	0.459
3	TOP	350	1650	0.15	0.926
	SIDE	350	1650	0.15	0.646

Hatch distance directly affects the porosity of the part because too wide hatch distance will cause insufficient overlapping of the melt resulting in high porosities. Large hatch distance leads to the formation of gaps between the scan tracks due to the lack of intra-layer bonding.When the hatch distance increases, the intra-layer overlap diminishes and the part is held together mainly through inter-layer bonding. This inter-layer bonding given the cylindrical or segmental shape of the individual melt pools [13].

The hatch distance were set to be 0.13mm, it gives the smallest porosity percentage which is 0.53% and 0.46% compared to hatch distance of 0.1mm which is 1.26% and 1.48%. The hatch distance were increased to 0.15mm and shows slightly incresed in its porosity which is 0.93% and 0.65%.

Figure 5 shows the images obtained by optical microscope. The image shows the average size and distribution of metallurgical pores on the surface of the samples. Metallurgical pores, also known as hydrogen porosity, are spherically shaped and small in size (less than 100 µm) happens when the gases being trapped within the melt pool or evolving from the powder during consolidation. The images also shows that the porosity were high in the side surface compared to the top surface for the first set, while in the second and third sets, the porosity were high in the top surface compared to the side surface. Closer look were shown in figure 6, of both top and side surface by using optical microscope after electro-etched.

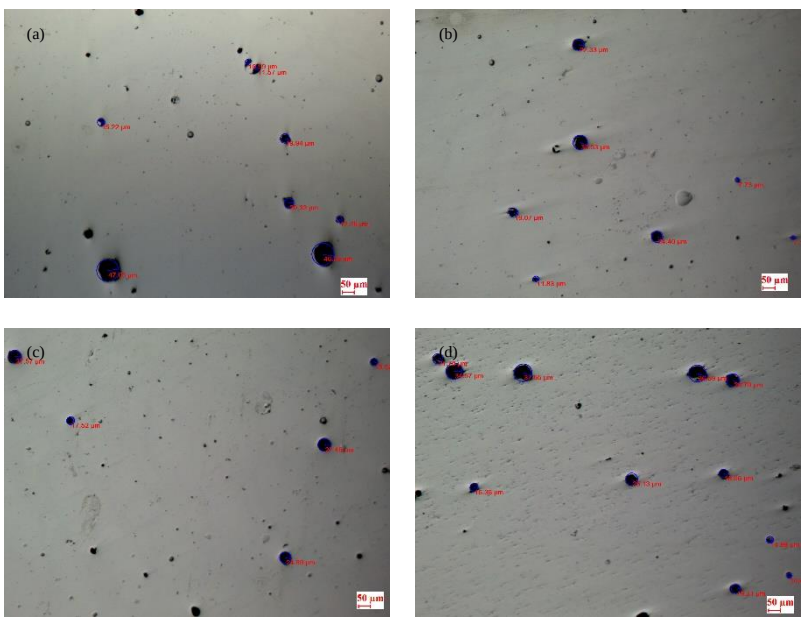

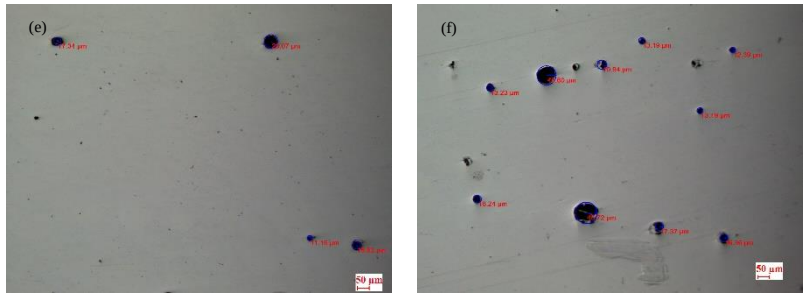

FIGURE 5: Evolution of pores with Hatch Distance: (a) 0.10mm, (b) 0.13mm, (c) 0.15mm on top surface of samples, (d) 0.10mm, (e) 0.13mm, (f) 0.15mm on side surface of samples.

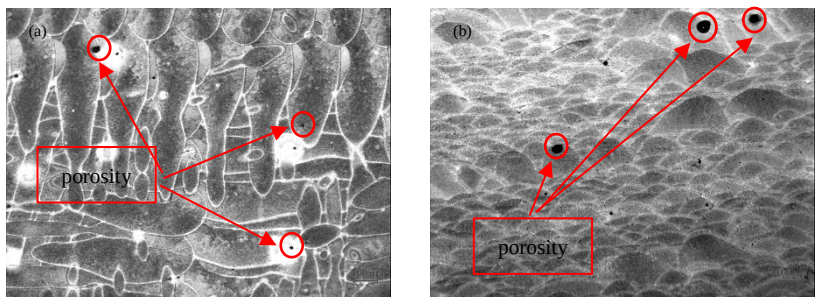

FIGURE 6: Optical image of (a) top surface (b) side surface with hatch distance of 0.13mm after electro-etching.

3. Conclusions

(a) The hatch distance controls the overlap between the scan tracks and affect the porosity of SLM-processed AlSi10Mg-alloy samples the most.

(b) Surveying the windows of parameters, the best combination was found to be laser power of 350 W, scanning speed of 1650 mm/s, and hatch distance of 0.13mm, and when using a layer thickness of 30μm. The lowest hatching distance in this study (0.10mm) were not suitable for such parameter setting (Laser power 350W and scanning speed 1650mm/s).

(c) Microscopic observations show that porosities are very small, on the order of 5 µm to 50 µm. However it cannot be neglected as it affects the density and mechanical properties of the SLM samples.

(d) Porosity in these samples was found to be made up entirely of only metallurgical pores with no evidence of keyhole pores in any of them as shown in Figure 5.

(e) No solidification cracks were observed, which was expected as AlSi10Mg alloy has a generally low crack sensitivity.

4. Acknowledgment

This research work is financially supported by Research Innovation Commercialization and Consultancy Management (ORICC), University Tun Hussein Onn Malaysia (UTHM).

5. References

[1] L. Z. Alexander, "Developing Process Capabilities for Selective Laser Melting," 2013.

[2] K. G. Prashanth, S. Scudino, H. J. Klauss, K. B. Surreddi, L. Löber, Z. Wang, A. K. Chaubey, U. Kühn, and J. Eckert, "Microstructure and mechanical properties of Al-12Si produced by selective laser melting: Effect of heat treatment," *Mater. Sci. Eng. A*, vol. 590, pp. 153–160, 2014.

[3] N. T. Aboulkhair, N. M. Everitt, I. Ashcroft, and C. Tuck, "Reducing porosity in AlSi10Mg parts processed by selective laser melting ☪," *Addit. Manuf.*, vol. 1–4, pp. 77–86, 2014.

[4] L. Thijs, K. Kempen, J. P. Kruth, and J. Van Humbeeck, "Fine-structured aluminium products with controllable texture by selective laser melting of pre-alloyed AlSi10Mg powder," *Acta Mater.*, vol. 61, no. 5, pp. 1809–1819, 2013.

[5] U. Tradowsky, J. White, R. M. Ward, N. Read, W. Reimers, and M. M. Attallah, "Selective laser melting of AlSi10Mg : In fl uence of post-processing on the microstructural and tensile properties development," *JMADE*, vol. 105, pp. 212–222, 2016.

[6] W. Li, S. Li, J. Liu, A. Zhang, Y. Zhou, Q. Wei, C. Yan, and Y. Shi, "Effect of heat treatment on AlSi10Mg alloy fabricated by selective laser melting: Microstructure evolution, mechanical properties and fracture mechanism," *Mater. Sci. Eng. A*, vol. 663, pp. 116–125, 2016.

[7] A. A. Raus, M. S. Wahab, M. Ibrahim, K. Kamarudin, A. Ahmed, and S. Shamsudin, "Mechanical and Physical Properties of AlSi10Mg Processed through Selective Laser Melting."

[8] E. O. Olakanmi, R. F. Cochrane, and K. W. Dalgarno, "A review on selective laser sintering/melting (SLS/SLM) of aluminium alloy

powders: Processing, microstructure, and properties," *Prog. Mater. Sci.*, vol. 74, pp. 401–477, 2015.

[9] G. Kasperovich, J. Haubrich, J. Gussone, and G. Requena, "Correlation between porosity and processing parameters in TiAl6V4 produced by selective laser melting," *JMADE*, vol. 105, pp. 160–170, 2016.

[10] N. Read, W. Wang, K. Essa, and M. M. Attallah, "Selective laser melting of AlSi10Mg alloy: Process optimisation and mechanical properties development," *Mater. Des.*, vol. 65, pp. 417–424, 2015.

[11] G. Kasperovich, J. Haubrich, J. Gussone, and G. Requena, "Correlation between porosity and processing parameters in TiAl6V4 produced by selective laser melting," vol. 105, pp. 160–170, 2016.

[12] A. Ahmed, M. S. Wahab, A. A. Raus, and K. Kamarudin, "Effects of Selective Laser Melting Parameters on Relative Density of AlSi10Mg A.," vol. 8, no. 6, pp. 2552–2557, 2017.

[13] N. T. Aboulkhair, "Additive manufacture of an aluminium alloy : processing , microstructure , and mechanical properties," no. December, 2015.